

Understanding the QCD medium by the diffusion of charm quarks using a color string percolation model

Kangkan Goswami[✉], Dushmanta Sahu, and Raghunath Sahoo^{✉*}

Department of Physics, Indian Institute of Technology Indore, Simrol, Indore 453552, India

 (Received 29 June 2022; accepted 12 December 2022; published 3 January 2023)

We study the drag and diffusion coefficients of the charm quark in the deconfined matter produced in the ultrarelativistic collisions by taking the color string percolation model (CSPM) approach. CSPM, being a QCD-inspired model, can give us essential information about the hot and dense system produced in ultrarelativistic collisions. With information on the initial percolation temperature and percolation density, we estimate the relaxation time (τ_c), drag coefficient (γ), transverse momentum diffusion coefficient (B_0), and spatial diffusion coefficient (D_s) of a charm quark inside a deconfined medium. Finally, we compare the obtained results with lattice QCD and with various other theoretical models. Good agreement can be observed between the results obtained from CSPM and lattice QCD.

DOI: [10.1103/PhysRevD.107.014003](https://doi.org/10.1103/PhysRevD.107.014003)

I. INTRODUCTION

Heavy quarks, such as the charm and bottom quarks, can be used as essential probes to study the initial phase of the system's evolution in an ultrarelativistic collision [1–4]. As the charm and bottom quarks have very high masses compared to the lighter quarks, they are produced relatively early in the evolution of the system. The masses of the heavy quarks are significantly larger than that of the temperature of quark-gluon plasma (QGP), which means that the probability of the charm and bottom quarks getting created or annihilated during the deconfined phase is much less than that of the lighter quarks and gluons. As a result, the heavy quarks witness the entire space-time evolution of the system. These heavy quarks interact with the hot and dense medium formed in the ultrarelativistic collisions, because of which their momentum spectra get modified. However, these interactions do not completely thermalize heavy quarks with intermediate and high transverse momentum (p_T). Thus, they can carry important information about the initial stages of the expanding fireball.

The energy loss mechanism of the heavy quarks in the medium is very distinct from that of the lighter quarks. For light quark jets, the leading mechanism for energy loss is due to the gluon radiation [5]. On the contrary, the gluon radiation mechanism will be suppressed for heavy quarks

[6], and their energy loss will be due mainly to the elastic collisions with the lighter quarks in the medium [7]. Moreover, the energy of a heavy quark is not changed too much from collisions with a light quark; thus, the thermalization time of the heavy quark will be substantially larger than that of the lighter quarks. It is worth mentioning that the QGP lifetime is estimated to be on the order of 4 to 5 fm/c [8] at the Relativistic Heavy Ion Collider (RHIC). Similarly, at the Large Hadron Collider (LHC), it is around 10–12 fm/c [9]. On the other hand, the thermalization time for a charm quark is calculated to be on the order of 10–15 fm/c, and for bottom quarks 25–30 fm/c [7,10,11]. The charm quark interaction with the thermalized lighter quarks and gluons in the medium will lead to a Brownian motion, which can be explained by the Fokker-Planck transport equation. Hence, information about the interaction of a heavy quark in the deconfined medium is preserved within its drag and diffusion coefficients, which can be estimated by solving the Fokker-Planck equation. While traversing through the medium, the average momentum of heavy quarks gets modified, which is incorporated into their drag coefficient. Their momentum distribution is also broadened and is embedded in their momentum diffusion coefficient. These coefficients vary with the temperature of the expanding matter, and, in principle, they can give essential information about the systems formed in high-energy collisions.

Apart from the drag and momentum diffusion coefficients, the spatial diffusion coefficient (D_s) is also of enormous interest to the scientific community. Theoretically, the heavy quark spatial diffusion coefficient has been calculated from perturbative QCD (pQCD) [12] and also from anti-de Sitter/conformal field theory (AdS/CFT) correspondence [13]. AdS/CFT calculations

*Corresponding author.
Raghunath.Sahoo@cern.ch

Published by the American Physical Society under the terms of the Creative Commons Attribution 4.0 International license. Further distribution of this work must maintain attribution to the author(s) and the published article's title, journal citation, and DOI. Funded by SCOAP³.

give the value of $2\pi TD_s = 1$ in the strong coupling limit [14]. As observed in several works in the literature, there is a minimum for this parameter approaching the AdS/CFT value near the critical temperature. In Ref. [15], Scardina *et al.* estimated the charm quark spatial diffusion coefficient from D meson spectra at energies available at RHIC and LHC. The heavy quark momentum and spatial diffusion coefficient have also been obtained from lattice QCD by investigating a color electric field correlation function using Monte Carlo techniques [16]. Recently, Brambilla *et al.* reported some progress toward the computation of a heavy quark momentum diffusion coefficient from two chromoelectric fields correlator attached to a Polyakov loop in $SU(3)$ gauge theory [17]. By studying the diffusion coefficient as a function of temperature, they show that the results from lattice QCD agree quite well with that of the next-to-leading-order perturbative results. The effect of viscosity on the diffusion coefficient has also been studied by taking a semi-QGP matrix model [18], where the spatial diffusion coefficient is observed to be decreasing with the increase in shear and bulk viscosities. In addition, the diffusion of a D meson in hot and dense hadronic matter has been studied for both zero and finite baryochemical potential cases [19]. A strong baryochemical potential dependency has been observed in the estimation of relaxation time for a D meson; for higher μ_B , the relaxation time is observed to be reduced by a factor of 2 to 3.

It has been observed that the color string percolation model (CSPM) can qualitatively explain the observed increase in the relative J/ψ yield with respect to relative charged-particle multiplicity in pp collisions at $\sqrt{s} = 7$ TeV [20]. This motivates us to look into heavy flavor dynamics in the deconfined medium by using the CSPM. In this work, we study the relaxation time, drag, and momentum diffusion coefficient of the charm quark, along with D_s as functions of the initial percolation temperature by taking the CSPM approach. The paper is organized as follows. Section II encompasses the CSPM framework along with the formalism of the drag and diffusion coefficients of the charm quark. In Sec. III, the results obtained using the formulation are discussed. Finally, Sec. IV concludes the findings of this study.

II. FORMULATION

A. Color string percolation model

The color string percolation model is a QCD-inspired, well-established model to explain the multiparticle production in an ultrarelativistic collision [21]. The model has been used to estimate various thermodynamic and transport properties of the matter formed in ultrarelativistic collisions, and the results have been found to be consistent with other existing models, such as lattice QCD [22–24]. In this model, the production of particles can be understood as a consequence

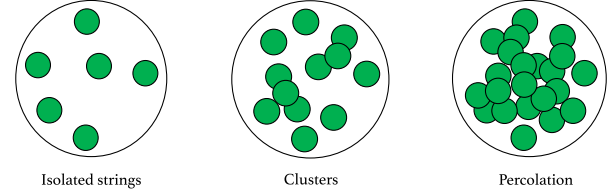


FIG. 1. Percolation of colored strings in the transverse space.

of color strings stretching between the partons of the target and the projectile. In transverse space, these strings occupy some finite area. With an increase in collision energy and the number of colliding partons, the number of strings grows, and they start to overlap, forming colored clusters in the transverse space. A macroscopic cluster appears after a certain critical string density (ξ_c), where 50% of the transverse space is occupied by the clusters. This marks the percolation phase transition [21], which is shown schematically in Fig. 1. According to Schwinger’s string breaking mechanism, these strings stretch and break to produce color-neutral quark and antiquark pairs. These particles finally hadronize to produce the final state hadrons [21].

In a 2D percolation theory, the total multiplicity due to an N_s number of overlapping strings is given as [25]

$$\mu_{N_s}/\mu_1 = \sum_{n=1}^{N_s} \sqrt{n}(S_n/S_1), \quad (1)$$

where n is any integer from 1 to N_s , S_1 is the transverse area of a single string given by $S_1 = \pi r_0^2$, with r_0 being the single string radius $\simeq 0.2$ fm, and S_n is the transverse area occupied by the overlapping strings.

Similarly, for the mean transverse momentum squared, $\langle p_T^2 \rangle$, we can write

$$\langle p_T^2 \rangle / \langle p_T^2 \rangle_1 = \frac{N_s}{\sum_{n=1}^{N_s} \sqrt{n}(S_n/S_1)}. \quad (2)$$

When the strings in the transverse plane are just touching each other such that $S_n = nS_1$, the total multiplicity and the mean transverse momentum squared changes as $\mu_n = n\mu_1$ and $\langle p_T^2 \rangle_n = \langle p_T^2 \rangle_1$, respectively. Another possible scenario is that all the strings overlap perfectly with each other such that $S_n = S_1$. In this case, we get $\mu_n = \sqrt{n}\mu_1$ and $\langle p_T^2 \rangle_n = \sqrt{n}\langle p_T^2 \rangle_1$. This gives us the case where the multiplicity is maximally suppressed and the mean transverse momentum squared is maximally enhanced. From this, we can write a relation between multiplicity and mean transverse momentum squared, $\mu_n \langle p_T^2 \rangle_n = n\mu_1 \langle p_T^2 \rangle_1$, which implies conservation of the total transverse momentum.

Now, assuming the transverse nuclear overlap area to be S and density ρ , we introduce a dimensionless percolation density parameter ξ given by [21]

$$\xi = \rho S_1 = \frac{N_s S_1}{S}. \quad (3)$$

In the thermodynamic limit, the number of strings $N_s \rightarrow \infty$ when ξ is fixed, and the distribution of the overlaps of n strings is Poissonian with a mean of value ξ ,

$$p_n = \frac{\xi^n}{n!} e^{-\xi}. \quad (4)$$

From the above expression, the fraction of the total area occupied by the strings can be given by,

$$\sum_{n=1} p_n = 1 - e^{-\xi}. \quad (5)$$

Dividing the above equation by ξ , we get the compression factor. Furthermore, according to the CSPM approach, the multiplicity becomes damped as a result of overlapping by the square root of the compression factor, which can be written as

$$\mu_n/\mu_1 = N_s \sqrt{\frac{1 - e^{-\xi}}{\xi}}. \quad (6)$$

Hence, the damping factor or the color suppression factor is finally given as [21]

$$F(\xi) = \sqrt{\frac{1 - e^{-\xi}}{\xi}}. \quad (7)$$

In ultrarelativistic heavy-ion collisions, thermalization can occur through the Hawking-Unruh effect [26,27], where fast thermalization happens with the existence of an event horizon caused by the rapid deceleration of the colliding nuclei [28]. In the CSPM, the intense color field inside the large cluster causes deceleration of the $q\bar{q}$ pair, which can be perceived as a thermal temperature due to the Hawking-Unruh effect. This suggests that the radiation temperature can be determined by the transverse extension of the color flux tube in terms of the string tension.

The initial temperature of the percolation cluster is expressed in terms of $F(\xi)$. The Schwinger distribution for massless particles can be expressed in terms of p_T^2 as [21,29–31]

$$dn/dp_T^2 \sim \exp(-\pi p_T^2/x^2), \quad (8)$$

where $\langle x^2 \rangle$ is the average value of string tension. As the chromoelectric field is not constant, the tension of the macroscopic cluster fluctuates around its mean value. Owing to these fluctuations, we get a Gaussian distribution of the string tension that is given as

$$\frac{dn}{dp_T^2} \sim \sqrt{\frac{2}{\langle x^2 \rangle}} \int_0^\infty dx \exp\left(-\frac{x^2}{2\langle x^2 \rangle}\right) \exp\left(-\pi \frac{p_T^2}{x^2}\right), \quad (9)$$

which in turn gives rise to a thermal distribution,

$$\frac{dn}{dp_T^2} \sim \exp\left(-p_T^2 \sqrt{\frac{2\pi}{\langle x^2 \rangle}}\right). \quad (10)$$

From Eqs. (8) and (10), the initial temperature in terms of $F(\xi)$ can be expressed as [31–33]

$$T(\xi) = \sqrt{\frac{\langle p_T^2 \rangle_1}{2F(\xi)}}, \quad (11)$$

where $\langle x^2 \rangle = \pi \langle p_T^2 \rangle_1 / F(\xi)$. By using $T_c = 167.7 \pm 2.8$ MeV [34,35] and $\xi_c \sim 1.2$ [21], we can get the single string squared average transverse momentum, $\sqrt{\langle p_T^2 \rangle_1} = 207.2 \pm 3.3$ MeV. Using this value in Eq. (7), we can get the initial temperature for different $F(\xi)$ values. With this information, let us estimate the drag and diffusion coefficients within the CSPM formalism.

B. Drag and diffusion coefficients

To study the interaction of a charm quark with the thermal quarks inside the deconfined medium, we take advantage of the Fokker-Planck transport equation, which can be written as

$$\frac{\partial f(t, p)}{\partial t} = \frac{\partial}{\partial p^i} \left[(A^i f(t, p)) + \frac{\partial}{\partial p^j} (B^{ij} f(t, p)) \right]. \quad (12)$$

Here, $f(t, p)$ is the time evolution phase-space distribution of charm quarks. The kernels A^i and B^{ij} are given by [19]

$$A^i = \int dk \omega(p, k) k^i, \quad (13)$$

$$B^{ij} = \frac{1}{2} \int dk \omega(p, k) k^i k^j, \quad (14)$$

where $\omega(p, k)$ is the collision rate of the charm quark, with initial momenta p and final momenta $(p - k)$, with the transferred momenta k . $i, j = 1, 2, 3$ are the spatial indices. In the low transverse momentum limit ($p \rightarrow 0$), the kernels reduce to [19]

$$A_i = \gamma p_i, \quad (15)$$

$$B_{ij} = B_0 P_{ij}^\perp + B_1 P_{ij}^\parallel, \quad (16)$$

where γ is the drag coefficient, B_0 is the transverse momentum diffusion coefficient, and B_1 is the longitudinal momentum diffusion coefficient. P_{ij}^\parallel and P_{ij}^\perp are the

longitudinal and transverse projection operators, respectively. This drag and diffusion coefficient definition is valid only when the transferred energy is small. This is possible in the case of a charm quark being nonrelativistic. The NRQCD model assumes the heavy particles to be nonrelativistic, and it describes the inclusive production and decay of quarkonia along with the S -wave charmonium production at high transverse momentum [36]. In line with this, we can assume the charm quark inside the deconfined medium to be nonrelativistic. Thus, the assumptions of Eqs. (15) and (16) hold true in this case.

The average momentum of a particle at a given time is given by [37]

$$\langle p \rangle = \frac{\int_{-\infty}^{\infty} dp p f(t, p)}{\int_{-\infty}^{\infty} dp f(t, p)} = p_0 e^{-\frac{t}{\tau}}, \quad (17)$$

where τ is the relaxation time and p_0 is the initial momentum of the particle. Relaxation time of a quark in the hot QCD medium is defined as the time accounting for the exponential decay of the average momentum. In other words, the average time interval between two successive collisions can be termed as the relaxation time of the system. Assuming the velocity of the thermal quarks to be nearly the speed of light, in natural units we can take the relaxation time to be equal to the mean free path of the system. The mean free path (λ) is inversely proportional to the number density (n) of the system and the scattering cross section (σ) between the particles [21,33],

$$\lambda = \frac{1}{n\sigma}. \quad (18)$$

In CSPM formalism, the number density is expressed as the effective number of color sources per unit volume,

$$n = \frac{N_{\text{sources}}}{SL}, \quad (19)$$

where S is the nuclear overlap area and L is the longitudinal extension of a string ~ 1 fm. This string length is chosen because no new quark-antiquark pairs can form if the separation between the gluons is less than 1 fm. In addition, the colliding nuclei are Lorentz contracted, making their longitudinal dimensions almost negligible. Thus, we take the lower limit of the string length, which is standard in CSPM studies.

The number of color sources can be defined as the transverse area occupied by the strings divided by the area of an effective string,

$$N_{\text{sources}} = \frac{(1 - e^{-\xi})S_N}{S_1 F(\xi)}. \quad (20)$$

Thus, the number density becomes

$$n = \frac{(1 - e^{-\xi})}{S_1 F(\xi)L}. \quad (21)$$

The cross section (σ) can also be expressed as the transverse area of the effective strings $S_1 F(\xi)$. Finally, using Eqs. (18) and (21) we can write

$$\lambda = \frac{L}{(1 - e^{-\xi})}. \quad (22)$$

Equation (22) can be used to define the relaxation time of the deconfined medium, $\tau = \lambda$ [38].

Now, for heavier quarks like charm quarks, the particle dependent relaxation time can be expressed as [39]

$$\tau_c = \frac{m_c}{T} \tau \quad (23)$$

$$\Rightarrow \tau_c = \frac{m_c}{T} \frac{L}{(1 - e^{-\xi})}, \quad (24)$$

where m_c is the mass of the charm quark, $m_c \simeq 1.275$ GeV. Owing to the dependency of the relaxation time on the mass of the particle, at any temperature, we expect the relaxation time of the charm quark to be significantly higher than that of the lighter quarks. This in turn affects the elliptic flow of a charm quark to be smaller than that of the light hadrons [12,15].

The drag coefficient or drag force (γ), which incorporates the average momentum change, is inversely related to the thermal relaxation time of the particle, $\gamma = \frac{1}{\tau_c}$. From the Einstein's relation, the transverse momentum diffusion coefficient for charm quarks, which accounts for broadening of the final momentum distribution, is related to the drag coefficient as [40]

$$B_0 = \gamma T m_c \quad (25)$$

$$\Rightarrow B_0 = \frac{(1 - e^{-\xi})T^2}{L}. \quad (26)$$

The diffusion coefficient (D_s) in position space can also be introduced. It can be estimated by starting a particle at position and time $x = 0$ and $t = 0$ and finding the mean squared position at a later time [37],

$$\langle (x(t) - x(0))^2 \rangle = 2D_s t. \quad (27)$$

Here, we can see that D_s is the measure of speed of diffusion in space and is called the ‘‘Einstein relation.’’ In static limit, the spatial diffusion coefficient is given by the expression [37,41]

$$D_s = \frac{T}{m_c \gamma} \quad (28)$$

$$\Rightarrow D_s = \frac{L}{(1 - e^{-\xi})}. \quad (29)$$

By taking inputs from the CSPM formalism and using the above formulation, we have estimated the relaxation time, drag, and diffusion coefficients of the charm quarks inside the deconfined medium, which are discussed in Sec. III.

III. RESULTS AND DISCUSSION

To better understand the systems produced in the ultra-relativistic collisions at RHIC and LHC, we have studied the relaxation time, drag, and diffusion coefficients of such matter using the CSPM. The results are contrasted with the results obtained from various other models. First, the charm quark relaxation time is plotted as a function of the initial temperature in Fig. 2. τ_c signifies the amount of time it takes for the charm particle to lose its total momentum by interaction with other quarks and gluons while traversing through the QGP medium. We observe that the relaxation time decreases with an increase in initial temperature. At temperatures nearing the critical value, the relaxation time of the charm quark is around 10 fm/c. With the rise in initial temperature the charm quark relaxation time decreases, and at 300 MeV it becomes about 4 fm/c. This is comparable with the result obtained in Ref. [12], where a pQCD approach has been taken considering resonant particles' inclusion inside the medium. The charm quark relaxation time is lower for a denser system, such as the one formed in most central heavy-ion collisions. In comparison, τ_c is relatively higher for a less dense medium, such as the one formed in high multiplicity pp collisions or peripheral heavy-ion collisions. This is because the charm quark will thermalize faster in a denser medium than in a

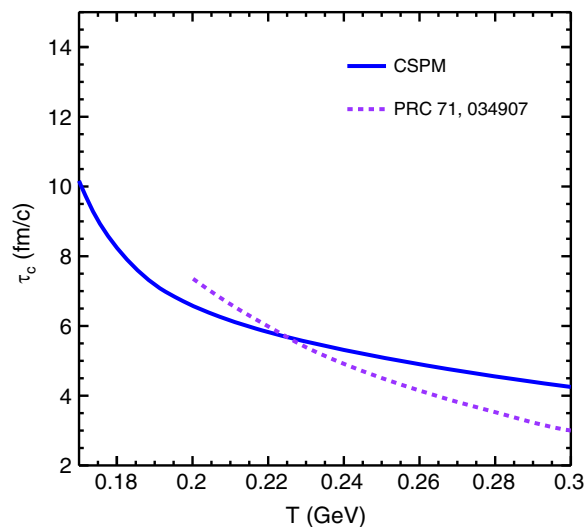


FIG. 2. Relaxation time of charm quarks as a function of the initial percolation temperature. The dotted violet line is from pQCD estimations with resonant particles [12].

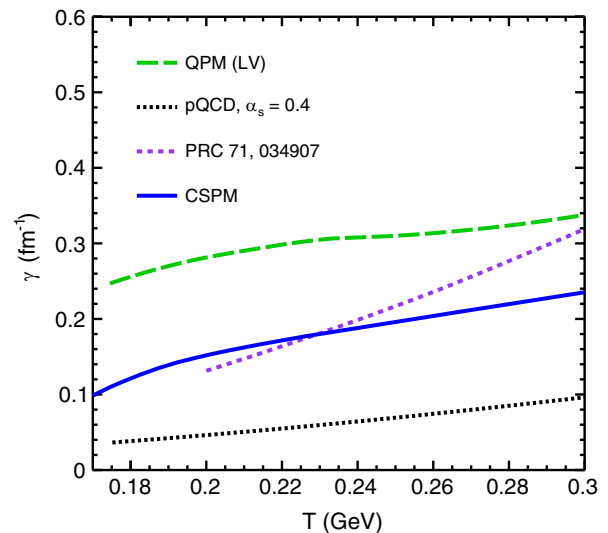


FIG. 3. Drag coefficient of charm quarks as a function of temperature. The dashed green line is from the quasiparticle model [15] and the dotted black and violet lines are from pQCD estimations without and with the inclusion of resonant particles, respectively [12].

less dense one due to substantially more interactions in the medium.

By taking input from the charm quark relaxation time, we estimate the drag force of the charm quark inside the medium, which is the inverse of the relaxation time. Figure 3 shows the drag force or drag coefficient of charm quark in the deconfined medium as a function of temperature. We observe an increasing trend with an increase in temperature. This suggests that the drag on the charm quark in denser systems, such as those produced in most central heavy-ion collisions, will be more than that in the peripheral collisions. For comparison, we have also plotted the drag force of charm quark estimated from the quasiparticle model [15] and pQCD [12]. The drag coefficient calculated from the quasiparticle model is a little higher than the CSPM estimation, whereas γ obtained from pQCD lies below the CSPM results. But there is a considerable agreement between the CSPM and the pQCD results with the inclusion of resonant particles inside the medium [12].

From Einstein's relation, the drag and momentum diffusion coefficients are related by Eq. (25). Figure 4 shows the transverse momentum diffusion coefficient as a function of temperature. We observe that B_0 increases linearly with an increase in temperature, suggesting that, at high temperatures, the momentum broadening of the charm quarks will be higher. We have also plotted the transverse momentum diffusion coefficient from pQCD to compare our results. The charm quark momentum diffusion from CSPM estimation is substantially larger than that of the pQCD calculation. This momentum diffusion of charm quarks, in principle, can affect the elliptic flow of the final state charmed hadrons. It is worth noting that, in the

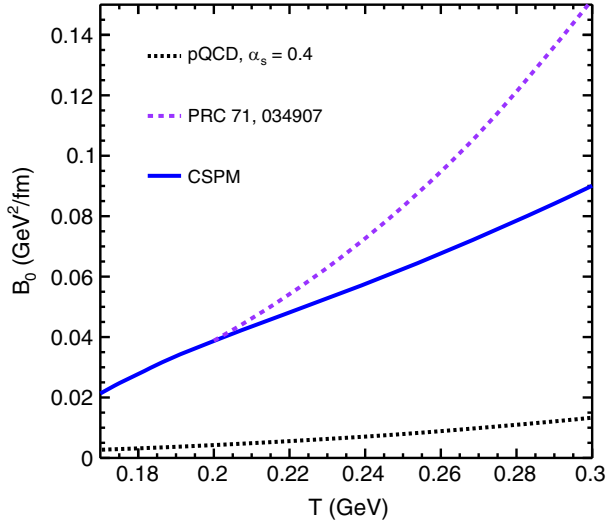


FIG. 4. Transverse momentum diffusion coefficient of charm quark as a function of temperature. The dotted black and violet lines are from pQCD estimations without and with the inclusion of resonant particles, respectively [12].

hadronic medium, D_0 meson will diffuse considerably larger than J/ψ [42]. This essentially results in a suppressed v_2 of D_0 . But, because J/ψ remains largely undiffused in the hadronic phase, the elliptic flow of J/ψ will give unfiltered information about the deconfined phase, making J/ψ a cleaner probe for studying QGP.

Finally, in Fig. 5 we have plotted the spatial diffusion coefficient as a function of temperature scaled with the

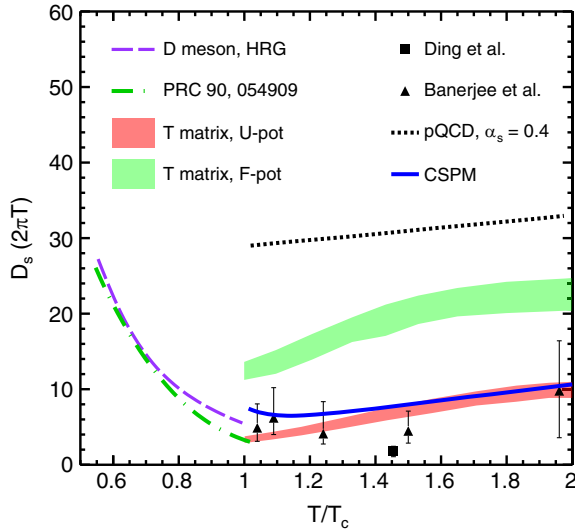


FIG. 5. The spatial diffusion coefficient as a function of temperature scaled with critical temperature. The red and green bands are the results obtained from T -matrix calculations for a U pot and an F pot, respectively [43]. The black dotted line is from pQCD calculations [12], the triangle [16], and rectangle [44] markers are from lattice QCD estimations. The violet dashed line [45] and the dash-dotted green line [19] are the results from D meson diffusion in a hadron gas.

critical temperature. Expressing the transport coefficients in units of thermal wavelength is very convenient; thus, we have multiplied a factor of $(2\pi T)$, making the diffusion coefficient dimensionless. This dimensionless quantity can characterize the coupling strength of the charm quark to the thermal medium. We have compared our results with various other results that already exist in the literature, such as estimations from T -matrix [43], pQCD [12], and lattice QCD [16,44] calculations. Interesting results have also been observed from the D meson diffusion in the hadron gas [19,45]. As the temperature approaches T_c , the D meson diffusion decreases rapidly and is almost comparable with that of the charm quark diffusion values at the critical temperature, showing almost a smooth transition from hadronic to partonic phase. From AdS/CFT calculations, the shear viscosity-to-entropy density ratio gives the minimum value of $1/4\pi$ [46]. When we study the change of η/s with temperature [22], we observe that η/s decreases with an increase in temperature and becomes minimum at $T = T_c$, and then again starts increasing with temperature. In addition, from the study of ζ/s as a function of temperature [22], we observe that at $T = T_c$ the bulk viscosity-to-entropy density becomes minimum and almost close to zero. Similarly, AdS/CFT calculation gives a minimum of $D_s(2\pi T) \sim 1$ [14] at the critical temperature. In Fig. 5 we can see that the value of $D_s(2\pi T)$ approaches this minima near T_c . Furthermore, we observe good agreement between the CSPM and other model estimations.

This behavior of the spatial diffusion coefficient can be understood in terms of the interaction strength in the system. In the hadronic phase, at a lower temperature, the interaction will be less; thus, the spatial diffusion coefficient is higher. As the temperature increases and we go toward the critical temperature, the interaction also increases, resulting in lower values of $D_s(2\pi T)$. At $T = T_c$, the interaction will be maximum due to the onset of the QGP medium, which corresponds to the minimum of $D_s(2\pi T)$. After this, the spatial diffusion coefficient increases again with an increase in temperature. This is because, at a higher temperature, the patrons will be asymptotically free, resulting in a lower interaction strength.

IV. CONCLUSION

In this work, for the first time, we study the relaxation time, drag, and diffusion coefficients of charm quark in the deconfined medium by taking the color string percolation approach. Our result is comparable with the pQCD approach, where the resonant heavy-light quark interactions are introduced. The observations from the spatial diffusion coefficient state that there is a minimum at the phase transition. We observe that our findings from the CSPM agree with the results obtained from lattice QCD for the spatial diffusion coefficient.

In view of ALICE Run 3 going toward high luminosity, the heavy flavor sector will be of particular interest. With higher statistics, the study of hadron production containing charm and bottom quarks can be done with high precision for a broad multiplicity range. Our work, along with other theoretical works, will hopefully help us to understand heavy flavor dynamics in ultrarelativistic collisions as case studies.

ACKNOWLEDGMENTS

K. G. acknowledges the doctoral fellowship from UGC, Government of India. The authors gratefully acknowledge the DAE-DST, Government of India, funding under the megascience project “Indian participation in the ALICE experiment at CERN” bearing Project No. SR/MF/PS-02/2021-IITI (E-37123).

-
- [1] Y. Xu, M. Nahrgang, J. E. Bernhard, S. Cao, and S. A. Bass, *Nucl. Phys.* **A967**, 668 (2017).
- [2] F. Prino and R. Rapp, *J. Phys. G* **43**, 093002 (2016).
- [3] G. Aarts, J. Aichelin, C. Allton, R. Arnaldi, S. A. Bass, C. Bedda, N. Brambilla, E. Bratkovskaya, P. Braun-Munzinger, G. E. Bruno *et al.*, *Eur. Phys. J. A* **53**, 93 (2017).
- [4] V. Greco, *Nucl. Phys.* **A967**, 200 (2017).
- [5] R. Baier, Y. L. Dokshitzer, A. H. Mueller, S. Peigne, and D. Schiff, *Nucl. Phys.* **B483**, 291 (1997).
- [6] Y. L. Dokshitzer and D. E. Kharzeev, *Phys. Lett. B* **519**, 199 (2001).
- [7] G. D. Moore and D. Teaney, *Phys. Rev. C* **71**, 064904 (2005).
- [8] U. W. Heinz, *Nucl. Phys.* **A721**, C30 (2003).
- [9] P. Foka and M. A. Janik, *Rev. Phys.* **1**, 154 (2016).
- [10] H. van Hees, V. Greco, and R. Rapp, *Phys. Rev. C* **73**, 034913 (2006).
- [11] S. Cao and S. A. Bass, *Phys. Rev. C* **84**, 064902 (2011).
- [12] H. van Hees and R. Rapp, *Phys. Rev. C* **71**, 034907 (2005).
- [13] S. S. Gubser, *Phys. Rev. D* **76**, 126003 (2007).
- [14] P. Kovtun, D. T. Son, and A. O. Starinets, *J. High Energy Phys.* **10** (2003) 064.
- [15] F. Scardina, S. K. Das, V. Minissale, S. Plumari, and V. Greco, *Phys. Rev. C* **96**, 044905 (2017).
- [16] D. Banerjee, S. Datta, R. Gavai, and P. Majumdar, *Phys. Rev. D* **85**, 014510 (2012).
- [17] N. Brambilla, V. Leino, P. Petreczky, and A. Vairo, *Phys. Rev. D* **102**, 074503 (2020).
- [18] B. Singh and H. Mishra, *Phys. Rev. D* **101**, 054027 (2020).
- [19] V. Ozvenchuk, J. M. Torres-Rincon, P. B. Gossiaux, L. Tolos, and J. Aichelin, *Phys. Rev. C* **90**, 054909 (2014).
- [20] E. G. Ferreira and C. Pajares, *Phys. Rev. C* **86**, 034903 (2012).
- [21] M. A. Braun, J. Dias de Deus, A. S. Hirsch, C. Pajares, R. P. Scharenberg, and B. K. Srivastava, *Phys. Rep.* **599**, 1 (2015).
- [22] D. Sahu and R. Sahoo, *J. Phys. G* **48**, 125104 (2021).
- [23] A. N. Mishra, D. Sahu, and R. Sahoo, *Physics* **4**, 315 (2022).
- [24] D. Sahu, S. Tripathy, R. Sahoo, and S. K. Tiwari, *Eur. Phys. J. A* **58**, 78 (2022).
- [25] M. A. Braun and C. Pajares, *Eur. Phys. J. C* **16**, 349 (2000).
- [26] S. W. Hawking, *Commun. Math. Phys.* **43**, 199 (1975); **46**, 206(E) (1976).
- [27] W. G. Unruh, *Phys. Rev. D* **14**, 870 (1976).
- [28] P. Castorina, D. Kharzeev, and H. Satz, *Eur. Phys. J. C* **52**, 187 (2007).
- [29] C. Y. Wong, *Introduction to High-Energy Heavy-Ion Collisions* (World Scientific, Singapore, 1994), p. 289.
- [30] J. S. Schwinger, *Phys. Rev.* **128**, 2425 (1962).
- [31] R. P. Scharenberg, B. K. Srivastava, and C. Pajares, *Phys. Rev. D* **100**, 114040 (2019).
- [32] A. N. Mishra, G. Paić, C. Pajares, R. P. Scharenberg, and B. K. Srivastava, *Eur. Phys. J. A* **57**, 245 (2021).
- [33] P. Sahoo, S. K. Tiwari, S. De, R. Sahoo, R. P. Scharenberg, and B. K. Srivastava, *Mod. Phys. Lett. A* **34**, 1950034 (2019).
- [34] P. Braun-Munzinger, J. Stachel, and C. Wetterich, *Phys. Lett. B* **596**, 61 (2004).
- [35] F. Becattini, P. Castorina, A. Milov, and H. Satz, *Eur. Phys. J. C* **66**, 377 (2010).
- [36] G. T. Bodwin, E. Braaten, and G. P. Lepage, *Phys. Rev. D* **51**, 1125 (1995); **55**, 5853(E) (1997).
- [37] J. M. Torres-Rincon, L. M. Abreu, D. Cabrera, F. J. Llanes-Estrada, and L. Tolos, *J. Phys. Conf. Ser.* **503**, 012020 (2014).
- [38] R. Rapp and H. van Hees, [arXiv:0803.0901](https://arxiv.org/abs/0803.0901).
- [39] P. Petreczky and D. Teaney, *Phys. Rev. D* **73**, 014508 (2006).
- [40] L. Tolos, J. M. Torres-Rincon, and S. K. Das, *Phys. Rev. D* **94**, 034018 (2016).
- [41] Goran Peskir, *Stoch. Models* **19**, 383 (2003).
- [42] S. Mitra, S. Ghosh, S. K. Das, S. Sarkar, and J.-e. Alam, *Nucl. Phys.* **A951**, 75 (2016).
- [43] F. Riek and R. Rapp, *Phys. Rev. C* **82**, 035201 (2010).
- [44] H. T. Ding, A. Francis, O. Kaczmarek, F. Karsch, H. Satz, and W. Soeldner, *Phys. Rev. D* **86**, 014509 (2012).
- [45] L. Tolos and J. M. Torres-Rincon, *Phys. Rev. D* **88**, 074019 (2013).
- [46] P. Kovtun, D. T. Son, and A. O. Starinets, *Phys. Rev. Lett.* **94**, 111601 (2005).